Environmental Science
Water Research & Technology

ROYAL SOCIETY OF CHEMISTRY

PAPER

View Article Online
View Journal | View Issue

Cite this: *Environ. Sci.: Water Res. Technol.*, 2021, **7**, 346

Optical properties and photochemical production of hydroxyl radical and singlet oxygen after ozonation of dissolved organic matter†

Frank Leresche, [ab] Jeremy A. Torres-Ruiz, [c] Tyler Kurtz, [a] Urs von Gunten [de] and Fernando L. Rosario-Ortiz *[ab]

Received 25th September 2020,
Accepted 23rd December 2020

DOI: 10.1039/d0ew00878h

rsc.li/es-water

This study focuses on the effects of ozonation on the optical and photochemical properties of dissolved organic matter (DOM). Upon ozonation, a decrease in light absorption properties of DOM was observed concomitantly with a large increase in singlet oxygen ($^1O_2$) and hydroxyl radical ($^{\bullet}OH$) quantum yields ($\Phi_{^1O_2}$ and $\Phi_{^{\bullet}OH}$, respectively). The decrease in absorbance was linked to the reaction of DOM chromophores with ozone and $^{\bullet}OH$, formed as a secondary oxidant, while the increase in $\Phi_{^1O_2}$ and $\Phi_{^{\bullet}OH}$ are linked to the formation of quinone-like moieties from the reaction of ozone with phenolic DOM moieties. Investigations using benzoic acid as a $^{\bullet}OH$ probe and methanol as a $^{\bullet}OH$ scavenger indicated that not only is $^{\bullet}OH$ formed, but that other hydroxylating species ($^{\bullet}OH$-like) are also produced upon DOM photo-irradiation.

Water impact

Water treatment tends towards increasingly numerous treatment steps. A better understanding of the effects of ozonation on the optical and photochemical properties of dissolved organic matter is necessary to optimize treatment processes. Ozonation induces a decrease in light absorbance and can help downstream UV-based treatment steps or for wastewater leads to improvements of the aesthetics of the water.

Introduction

Ozonation is a process widely applied in drinking water treatment and more recently also as a polishing step in secondary effluents of municipal wastewater treatment plants.[1,2] In addition to its use as a disinfectant and for the oxidation of micropollutants, ozone reacts with the dissolved organic matter (DOM) present in the water, leading to changes in its physico-chemical properties.[3–5] Because wastewater is usually discharged to a receiving water body (*e.g.*, river, lake, sea) and can represent an important fraction of the receiving water, ozone-induced transformations of DOM are of interest.[6,7]

DOM plays an important role in the photo-transformation of contaminants in surface waters by absorbing a portion of sunlight, thereby decreasing the direct photo-transformation of contaminants (eqn (1)), and by producing reactive intermediates (RI). These RI include excited triplet state of the DOM (^{3}DOM*, eqn (2)), singlet oxygen ($^1O_2$, eqn (3)) and hydroxyl radical ($^{\bullet}OH$, eqn (4), where DOM′ represents a transformed chromophore of DOM). The RI can react with contaminants leading to transformation products (eqn (5)).[8–12] Ozonation of DOM will affect this photochemistry by changing the light absorption properties of DOM and potentially affecting the yields of the RI.[3]

$$\text{Contamint} + h\nu \rightarrow \text{Products} \quad (1)$$

$$\text{DOM} + h\nu \rightarrow {}^1\text{DOM}^* \rightarrow {}^3\text{DOM}^* \quad (2)$$

$${}^3\text{DOM}^* + O_2 \rightarrow \text{DOM} + {}^1O_2 \quad (3)$$

$$\text{DOM} + h\nu \rightarrow \text{DOM}' + {}^{\bullet}OH \quad (4)$$

$$({}^1O_2 \text{ or } {}^3\text{DOM}^* \text{ or } {}^{\bullet}OH) + \text{Contaminant} \rightarrow \text{Products} \quad (5)$$

[a] *Environmental Engineering Program, University of Colorado Boulder, Colorado 80309, USA. E-mail: Fernando.rosario@colorado.edu*
[b] *Department of Civil, Environmental and Architectural Engineering, University of Colorado Boulder, Colorado 80309, USA*
[c] *Department of Chemistry, University of Puerto Rico, Mayagüez, Puerto Rico 00682, USA*
[d] *Eawag, Swiss Federal Institute of Aquatic Science and Technology, Überlandstrasse 133, CH-8600 Dübendorf, Switzerland*
[e] *School of Architecture, Civil and Environmental Engineering (ENAC), Ecole Polytechnique Fédérale de Lausanne (EPFL), CH-1015 Lausanne, Switzerland*
† Electronic supplementary information (ESI) available. See DOI: 10.1039/d0ew00878h

Studies have shown that ozonation of DOM leads to changes in its physicochemical properties, including decreases in light absorption, fluorescence intensity, chemical oxygen demand, and electron donating capacity, as well as the formation of low molecular weight compounds such as carboxylic acids and aldehydes.[1,3,4,13,14] DOM moieties have a large range of reactivity towards ozone. DOM moieties with high ozone reactivities are hypothetized to be mostly phenolic compounds that react to form quinones, ketones, catechol, and ring opening products.[15,16] Ozone reactions with DOM were covered in recent publications and we refer the reader to those for more information.[3,4] Reaction of ozone with DOM forms $^{\bullet}OH$ as a secondary oxidant that can further react with the DOM.[17–19] $^{\bullet}OH$ reacts with aromatic or conjugated DOM moieties by $^{\bullet}OH$ addition or with unsaturated moieties by $H^{\bullet}$ abstraction.[1] Typical second order rate constants for $^{\bullet}OH$ addition reactions are between 1–10 × 10^9 M^{-1} s^{-1} and are relatively higher than $H^{\bullet}$ abstraction reactions, with typical second order rate constants in the range of 0.1–1 × 10^9 M^{-1} s^{-1}.[20]

In a previous publication, we discussed the effects of ozone on the optical properties of DOM and its effect on the photochemical generation of $^1O_2$.[3] Specifically, it was shown that during ozonation in the presence of *t*-butanol to quench $^{\bullet}OH$ (formed *via* ozone decomposition), both the fluorescence and $^1O_2$ quantum yield ($\Phi_{^1O_2}$) increased concomitantly. The fluorescence quantum yield increased by 92–111% for increasing specific ozone doses from 0 to 1 $mmol_{O_3}$ $mmol_C^{-1}$. Similarly, the $\Phi_{^1O_2}$ increased by 273–844%. In this previous publication it was hypothesized that this was due to the preferential reactions of ozone with phenolic DOM moieties and low fluorescence chromophores. This hypothesis is based on the following observations: (1) ozone reacts towards DOM faster at high pH than at low pH.[4] This can be explained by the reaction of ozone towards phenolate being several orders of magnitude faster than towards phenols (*e.g.* $k_{O_3,phenolate}$ = 1.4 × 10^9 M^{-1} s^{-1} *vs.* $k_{O_3,phenol}$ = 1.3 × 10^3 M^{-1} s^{-1} (ref. 1)). (2) The aforementioned formation of quinones from ozonation of phenols. (3) The fact that phenols have low $\Phi_{^1O_2}$ (1–6%)[21] while quinones have generally higher $\Phi_{^1O_2}$ (20–98%).[22–25] (4) Low ozone doses can induce an increase in $^1O_2$ production rate.[3] It should be noted that ref. 3 attributes the observed increase in fluorescence quantum yield upon DOM ozonation to a preferential ozone reaction towards chromophores absorbing at long wavelengths that have low fluorescence quantum yields. Such preferential reactions of ozone with chromophores absorbing at long wavelengths may also explain part of the observed increase in $\Phi_{^1O_2}$. However, given the magnitude of the effect, it cannot be the sole explanation for the observed increase in $\Phi_{^1O_2}$.

The goal of this study was to expand on our earlier work and investigate the impact of ozone on the photochemical formation of $^{\bullet}OH$ from DOM. Specifically, this paper focuses on the effects of ozonation on (1) the optical properties of DOM, such as the absorbance spectra and of parameters that can be derived from the absorbance, and (2) the potential of DOM to generate singlet oxygen ($^1O_2$) and $^{\bullet}OH$ under simulated sunlight irradiation. In this study, we evaluated the impact of ozone without a $^{\bullet}OH$ quencher, therefore, providing a realistic depiction of the expected effects during the application of ozone in engineered systems. In addition to these effects of ozone, this paper also provides new insights on the molecular composition of DOM.

Materials and methods

Analytical instrumentation

UV-vis spectra and absorbance were measured on a Cary 100 Bio UV-visible spectrophotometer using 0.2, 1, or 5 cm pathlength quartz cuvettes. The pH was measured using a calibrated Orion Star A211 pH-meter using a Thermo Scientific Orion pH electrode model 8157BNUMD.

Following the photo-irradiation experiments, concentrations of the probe compounds and of the actinometer were measured in duplicate using an Agilent 1200 high-performance liquid chromatography (HPLC) system equipped with a UV-vis detector, a fluorescence detector and an Agilent Eclipse Plus C-18 5 μm particle size reverse phase column. Details of the applied isocratic method are provided in Table S1 (ESI†).

Chemicals and solutions

Chemicals were used as received except for *p*-nitroanisole (PNA), which was recrystallized in hexane, and benzoic acid (BA), which was recrystallized in water to remove some salicylic acid (SA) impurities from the commercially available product. For a complete list of chemicals, refer to Text S1 (ESI†). All solutions were prepared in ultrapure water (resistivity 18.2 MΩ cm) obtained from a Sartorius Stedim or equivalent dispenser. A 100 mM buffer stock solution was prepared by adding the appropriate amount of sodium phosphate salts. Diluted 1/10 v/v with water, it resulted in a 10 mM pH 7 phosphate buffer used for the experiments.

Two DOM isolates were selected from the International Humic Substance Society (IHSS, St-Paul, MN, USA) as representative of autochthonous (Pony Lake fulvic acid (PLFA), 1R109F) and allochthonous (Suwannee River fulvic acid (SRFA), 1S101F) DOM. The carbon content of the DOM solutions was measured spectrophotometrically using the specific ultraviolet absorbance value at the wavelength λ = 254 nm ($SUVA_{254}$) of 4.2 and 2.5 L mg_C^{-1} m^{-1} for SRFA and PLFA, respectively.[5] Stock solutions of the two DOM types were prepared at concentrations of ≈50 mg_C L^{-1} in pH 7 buffer. After stirring for 3–4 hours, the stock solutions were filtered by ultrapure water prewashed 0.45 μm pore size polyethersulfone filters (Whatman) and the carbon content was then measured spectrophotometrically.

Ozonation experiments

An ozone/oxygen gas mixture was obtained from an Ozone Solutions ozone generator model TG-40 and bubbled in a cooled (2 °C) 2 L cylindrical vessel filled with ultrapure water.

An aqueous ozone stock solution with an ozone concentration of ≈1 mM was obtained and was measured using a 0.2 cm path length quartz cuvette on the aforementioned spectrophotometer and a molar absorption coefficient value of 3200 M^{-1} cm^{-1} at λ = 260 nm.[1] The ozone solution was then added to buffered (pH 7, using the aforementioned phosphate buffer) DOM solutions (final concentration 5 mg_C L^{-1}) at various specific ozone doses (≤1 $mmol_{O_3}$ $mmol_C^{-1}$) and the solutions were kept for a minimum of 2 days at 4 °C to allow ozone to react to completion. The specific ozone doses were chosen to be similar to those used in drinking water or wastewater facilities.[26–29] It should be noted that for the specific ozone doses of 0.75 and 1 $mmol_{O_3}$ $mmol_C^{-1}$ only the UV-vis absorbance spectra are presented. These two doses have low absorbance values (<0.01 at λ = 350 nm) that could suffer from systematic errors on the absorbance measurements and we decided not to use them for further calculations.

Irradiation experiments

The methods to determine $^1O_2$ steady-state concentration ($[^1O_2]_{ss}$) and quantum yield ($\Phi_{^1O_2}$) are described elsewhere.[3] Briefly, $[^1O_2]_{ss}$ during photoirradiation of the ozonated DOM solutions was measured by spiking the solution with 22.5 μM of furfuryl alcohol (FFA) and 0.1 M of methanol (to quench $^{\bullet}OH$). At this FFA concentration, $^1O_2$ is mostly (≈99%) deactivated by collision with water and the presence of FFA does not affect but allows to determine the $[^1O_2]_{ss}$.[30] The solutions were then irradiated in 5 mL glass vials in a Rayonet photo-reactor model RPR-100 equipped with 16 RPR-3500A lamps that had an emission spectrum centered around 366 nm (see Fig. S1, ESI† for an emission spectrum of the lamps). 100 μL aliquots were taken at regular time intervals (total irradiation time ≈1 hour), diluted 1/1 (v/v) with ultrapure water and subsequently the FFA concentration was analyzed by HPLC. The abatement of FFA was fitted to a first-order kinetic model using the software Origin 2018. The steady-state concentration of $^1O_2$ ($[^1O_2]_{ss}$) during the experiments was determined using the second-order rate constant $k_{FFA,^1O_2}$ of (1.00 ± 0.04) × 10^8 M^{-1} s^{-1}.[31] $\Phi_{^1O_2}$ was then determined by dividing $[^1O_2]_{ss}$ by the rate of light absorption.

The experiments to determine the production rate of $^{\bullet}OH$ and the $\Phi_{^{\bullet}OH}$ where conducted similarly as for the determination of $^1O_2$ and are described in Text S2 (ESI†). Briefly, we spiked the samples with 1 mM of BA and the $^{\bullet}OH$ production was determined by following the zero-order production of SA from the reaction of BA with $^{\bullet}OH$ using the yield of the reaction of BA + $^{\bullet}OH$ → SA of 15.5%.[32] For the experiments that used both BA and methanol as $^{\bullet}OH$ probes, the experiment's irradiation time was relatively longer due to the overall lower rate of SA production and we observed a small (≈10% in control experiments containing the ozonated DOMs, 100 nM SA and 0.01 M methanol, irradiated for 225 minutes) degradation of SA during the experiments. The rate of SA production was calculated in these experiments by fitting the SA concentration to a zero-order production rate followed by a first-order degradation rate for SA. The corresponding equation is derived in Text S3 (ESI†) and an example of fitting is provided in Fig. S8 (ESI†).

Concomitantly to the FFA or BA irradiation experiments, we ran chemical actinometry daily to determine the irradiance of the lamps in the reactor. We used the PNA + pyridine actinometer at a concentration of 10 μM of PNA and of 5 mM of pyridine.[33] At this pyridine concentration, the quantum yield for the phototransformation of PNA (which depends on the pyridine concentration) is 1.74 × 10^{-3}.[34] All results were normalized by using the daily measured PNA phototransformation rate to the average PNA phototransformation value of 8.68 × 10^{-4} s^{-1}. The photon fluence rate in the interval λ = 340–410 nm was calculated to be of 1.40 × 10^{-3} Einstein m^{-2} s^{-1}.

Calculation of optical parameters

Optical parameters calculated from the UV-vis absorption spectra are often used because absorption spectra are easy to measure and the optical parameters correlate with DOM properties that are harder to measure such as $\Phi_{^1O_2}$ and $\Phi_{^{\bullet}OH}$. Several optical parameters were calculated using the measured UV-vis absorbance spectra of the solutions. The specific UV absorbance $SUVA_{254}$ (unit L mg_C^{-1} m^{-1}) was calculated by dividing the absorbance at the wavelength λ = 254 nm by the carbon concentration (5 mg_C L^{-1}). Fitting a single-parameter exponential regression to the absorbance spectra in the wavelength range 300–600 nm, the spectral slope (S, unit nm^{-1}) was calculated as the coefficient of the exponential fit (according to eqn (6)) using $Abs_{\lambda=350\ nm}$ as a constant. The *E2*/*E3* ratio was calculated as the ratio of the absorbance values at the wavelengths λ = 250 over λ = 365 nm. Both the spectral slope and the *E2*/*E3* ratio inversely correlate with the molecular weight of the DOM and positively correlate with $\Phi_{^1O_2}$ and $\Phi_{^{\bullet}OH}$.[35–37] The wavelength averaged specific absorption coefficient ($SUVA_{avg}$, unit L mg_C^{-1} m^{-1}), which is a proxy for the extent of light absorbed by the solutions, was calculated in the wavelength interval 340–410 nm according to eqn (7), where $SUVA_\lambda$ is the specific absorption coefficient at a wavelength λ (unit L mg_C^{-1} m^{-1}) and I_λ is the normalized photon irradiance of the Rayonet reactor.

$$Abs_\lambda = Abs_{\lambda=350nm} e^{-S(\lambda-350nm)} \quad (6)$$

$$SUVA_{avg} = \frac{\int_{340\,nm}^{410\,nm} SUVA_\lambda I_\lambda d\lambda}{\int_{340\,nm}^{410\,nm} I_\lambda d\lambda} \quad (7)$$

Standard deviation

The standard deviations were calculated for the first-order degradation curves of FFA and PNA and for the zero-order

production lines for SA and propagated from there. The error on the rate constants from the literature used in the calculations were also incorporated in the error calculation. The standard errors calculated for FFA degradation and SA production were used in addition to the standard errors for $SUVA_{avg}$ in the calculation of $\Phi_{^1O_2}$ and $\Phi_{\cdot OH}$. The standard errors for $SUVA_{avg}$ were calculated as the standard deviation of triplicate UV-vis absorbance measurements of the DOM solutions and propagated from there. Examples of calculations are shown in Text S4 (ESI†).

Results and discussion

Effects of ozonation on the optical properties of DOM

Absorption properties. As shown previously, ozonation induces a large decrease in the UV-vis absorption of the two DOM isolates tested in this study (Fig. 1). The allochthonous SRFA absorbs more light because it has a higher content of aromatic moieties than PLFA. While the absolute difference ($A_{O_3,dose=0} - A_{O_3,dose}$) of the absorbance is more important at shorter wavelengths

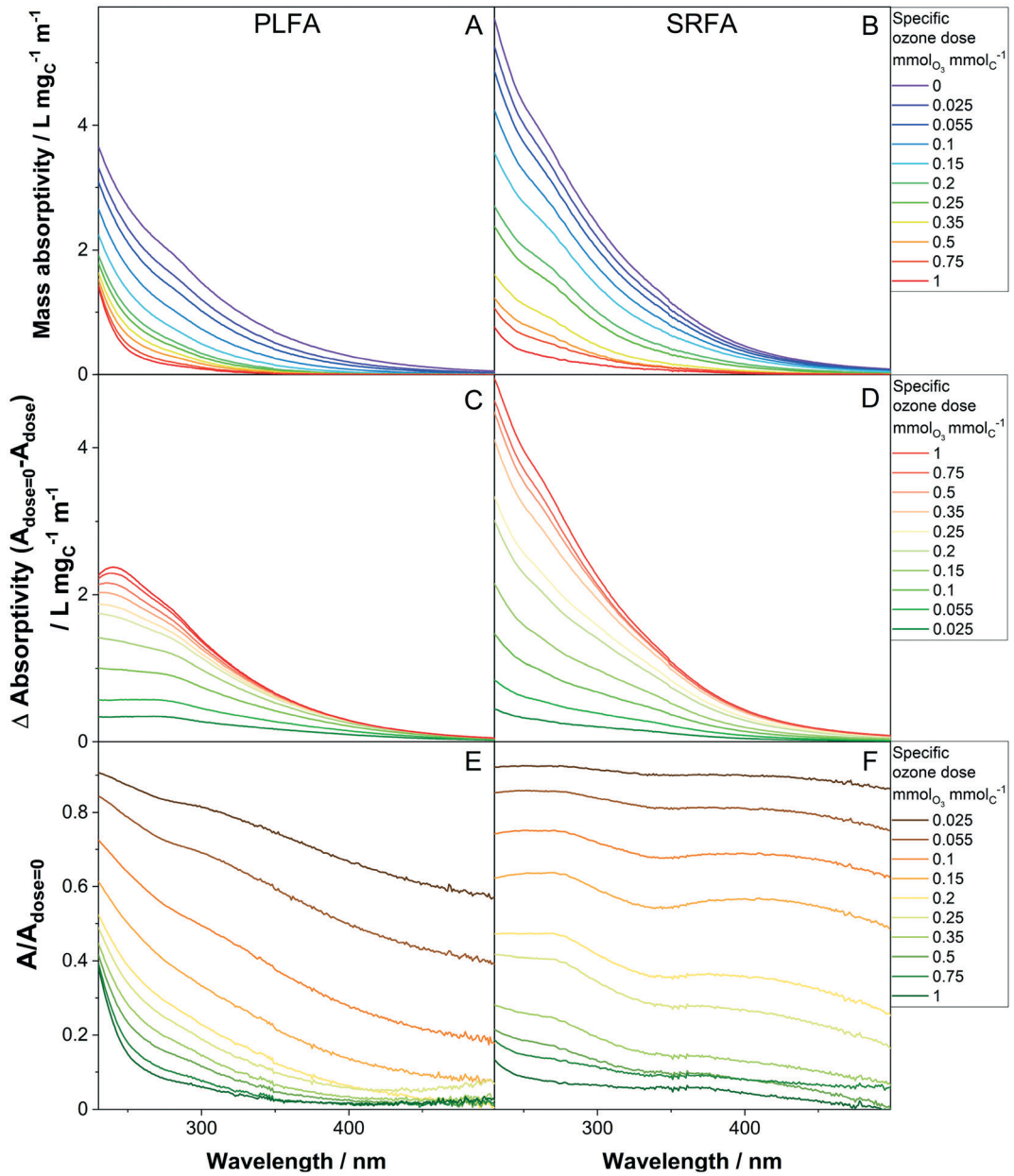

Fig. 1 Effects of the specific ozone doses on the absorbance spectra of the two DOM samples Pony Lake and Suwannee River fulvic acid (PLFA and SRFA respectively). (A) and (B): Mass absorptivity as a function of the specific ozone dose for (A) PLFA, and (B) SRFA. (C) and (D): Variation of the mass absorptivity ($A_{O_3,dose=0} - A_{O_3,dose}$) as a function of the specific ozone dose for (C) PLFA and (D) SRFA. (E) and (F): Ratio of the absorptivity $A_{O_3,dose}/A_{O_3,dose=0}$ as a function of the specific ozone dose for (E) PLFA and (F) SRFA. The samples were buffered at pH 7 using 10 mM phosphate buffer, with a DOM concentration of 5 $mg_C\ L^{-1}$.

(Fig. 1C and D), the relative decrease ($A_{O_3}/A_{O_3=0}$) in absorbance is smaller at shorter wavelengths (Fig. 1E and D). Upon ozonation, the relative decrease in absorbance ($A_{O_3}/A_{O_3=0}$) differs for the two DOM types (Fig. 1E and D). For PLFA, the relative decrease is more significant at longer wavelengths, whereas for SRFA the wavelength dependence is relatively small (see Fig. S2, ESI†). Typically, small ozone doses induce a large decrease in absorbance (Fig. 1 and S2, ESI†). For SRFA at λ = 254 nm, the absorbance decreases by 52% for a specific ozone dose of 0.2 $mmol_{O_3}$ $mmol_C^{-1}$ while for PLFA the decrease is 63%.

The observed effects of ozone on the absorption properties of DOM for specific ozone doses of up to 0.2 $mmol_{O_3}$ $mmol_C^{-1}$ are similar to a previous study conducted with the same DOM types in presence of a $^{\bullet}OH$ scavenger (as seen by similar reduction in $SUVA_{254}$, $SUVA_{280}$ and $SUVA_{350}$ values, see Fig. S3, ESI†)[3] and are similar to what was observed for three specific ozone doses for the same DOM types in the absence and presence of a $^{\bullet}OH$ scavenger.[5] These observations can be mainly rationalized by the reaction of ozone with highly reactive activated aromatic compounds such as phenols. For specific ozone doses >0.2 $mmol_{O_3}$ $mmol_C^{-1}$, the extent of $SUVA_{254}$ decrease was higher in the current study compared to our previous investigation.[3] This can be attributed to a depletion of the pool of highly ozone-reactive chromophores for specific ozone doses >0.2 $mmol_{O_3}$ $mmol_C^{-1}$ and the reactions of $^{\bullet}OH$ with these chromophores, which is possible due to the absence of a $^{\bullet}OH$ scavenger. Such chromophores can be non-activated aromatic moieties such as benzene or methylated benzenes, which have low second order rate constants for the reactions with ozone but are highly reactive towards $^{\bullet}OH$ ($k_{^{\bullet}OH,benzene}$ = 3.3 × 10^9 M^{-1} s^{-1}).[38] The reaction of benzene with $^{\bullet}OH$ produces phenol, which then reacts quickly with ozone.

Optical parameters. Optical parameters such as $SUVA_{254}$, the ratio *E2*/*E3*, and the spectral slope are often calculated from the UV-vis absorbance spectra for the characterization of waters.[35] In turn, these parameters are used to develop correlations with other reactivity measures of DOM, including the photochemical formation of $^1O_2$ or $^{\bullet}OH$ as well as other properties such as aromaticity and molecular weight.[37,39–41] Changes in these parameters are presented in Fig. S4 (ESI†) as a function of the specific ozone dose. A marked decrease in $SUVA_{254}$ with increasing specific ozone dose can be observed for both SRFA and PLFA (Fig. S4A, ESI†). In contrast, an increase in both the ratio *E2*/*E3* and the spectral slope can be observed for increasing specific ozone doses (Fig. S4B and C, ESI† respectively), being more pronounced for PLFA than for SRFA.

The results for ozonation in the presence and absence of an $^{\bullet}OH$ scavenger (*t*-butanol) also show that the decrease in $SUVA_{254}$ and the increases in *E2*/*E3* and the spectral slope are more important for PLFA in absence of an $^{\bullet}OH$ scavenger (Fig. S4, ESI†). For SRFA, $SUVA_{254}$ behaves similarly, however, for *E2*/*E3* and the spectral slope the observed increases are more pronounced in presence of the $^{\bullet}OH$ scavenger. The spectral slope PLFA results are in contradiction with the results presented in ref. 5 where the absence of the $^{\bullet}OH$ scavenger produced the opposite effect. The observed difference could be attributed to differences in the experimental conditions, with different DOM concentrations (10 mg_C L^{-1} in ref. 5 *vs.* 5 mg_C L^{-1} in the current study) and a difference in the way the ozonation experiments were conducted (in ref. 5 the residual ozone was quenched after 2 hours *vs.* 2 days in the present experiments).

As aforementioned, the $SUVA_{254}$, the ratio *E2*/*E3*, and the spectral slope correlate with $\Phi_{^{\bullet}OH}$ and $\Phi_{^1O_2}$. These correlations are presented in Fig. S5 and Table S2 (ESI†). The slopes of the $\Phi_{^1O_2}$ regressions (Fig. S5A–C, ESI†) are comparable (factor 2) to our previous study with the same isolates in the presence of a $^{\bullet}OH$ scavenger and to Everglades DOM (Table S2, ESI†).[3,37] The slopes of the $\Phi_{^{\bullet}OH}$ regressions in this study are significantly larger (by a factor of 2–6) than that of the Everglades DOM.[37] This observed difference in slope for the $\Phi_{^{\bullet}OH}$ regressions makes the direct use of any of the parameters ($SUVA_{254}$, the ratio *E2*/*E3*, and the spectral slope) as predictors of $\Phi_{^{\bullet}OH}$ questionable. The difference in slope may reflect a change in DOM chemical composition due to ozonation, as opposed to DOM composition of the Everglades DOM.

Effects of ozonation on the photochemical generation of $^1O_2$ from DOM. The extent of light absorbed in the wavelength interval 340–410 nm by the two DOM isolates can be characterized by $SUVA_{avg}$ as a proxy, which decreases in an exponential-like fashion upon ozonation (Fig. 2A). The steady-state concentration of $^1O_2$ produced upon UV irradiation (centered at λ = 366 nm, see Fig. S1, ESI†) increases slightly for low specific ozone doses (0 to 0.1 $mmol_{O_3}$ $mmol_C^{-1}$) and then decreases sharply (by a factor of 3) for PLFA and moderately for SRFA (Fig. 2B). Because $[^1O_2]_{ss}$ is decreasing relatively less compared to $SUVA_{avg}$ (Fig. 2A) it can be concluded that $\Phi_{^1O_2}$ (*i.e.*, the ratio of the production of $^1O_2$ over the extent of light absorption) should increase with increasing specific ozone doses. This is illustrated in Fig. 2C, where $\Phi_{^1O_2}$ increases close to linearly with increasing specific ozone doses. The increase in $\Phi_{^1O_2}$ is more significant for PLFA, with an increase from 1.9% (non-ozonated) to 13.1% (0.5 $mmol_{O_3}$ $mmol_C^{-1}$), than for SRFA for which an increase from 1.0 to 8.5% for the same specific ozone doses was observed.

Increases in $\Phi_{^1O_2}$ were similar in a previous study on wastewater ozonation[13] and in a study with the same DOM isolates but in the presence of a $^{\bullet}OH$ scavenger[3] (see Fig. S7, ESI† for a comparison with the data from ref. 3). The $\Phi_{^1O_2}$ values were 3.2 ± 0.4% for the non-ozonated wastewater and increased to 9.3 ± 1.8% for a

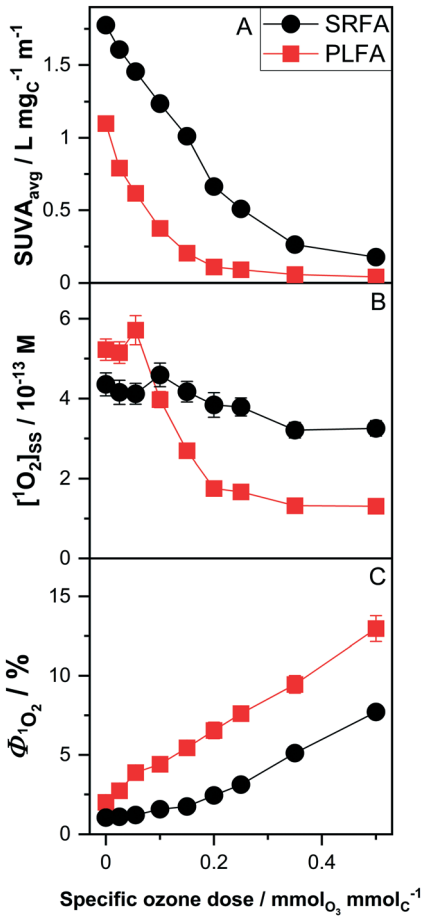

Fig. 2 Effects of specific ozone doses on (A) the light absorption, (B) the generation of singlet oxygen ($^1O_2$) and (C) the $^1O_2$ quantum yields ($\Phi_{^1O_2}$) for Pony Lake and Suwannee River fulvic acids (PLFA and SRFA, respectively). (A) Specific UV-vis absorption ($SUVA_{avg}$) in the wavelengths range 340–410 nm. (B) Measured steady-state $^1O_2$ concentration ($[^1O_2]_{ss}$) as a function of the specific ozone doses. (C) $^1O_2$ quantum yield ($\Phi_{^1O_2}$) as a function of the specific ozone dose. Red squares/lines: PLFA; black circles/lines: SRFA, at a concentration of 5 mg_C L^{-1}. Solutions were buffered with 10 mM phosphate at pH 7, without hydroxyl radical scavenger. Error bars represents standard errors in (B) and (C) were obtained from pseudo-first order fittings (FFA experiments in duplicate). Lines are shown to guide the eye.

specific ozone dose of 0.25 $mmol_{O_3}$ $mmol_C^{-1}$,[13] which is similar to the observations for PLFA. For ozonation of the same DOM isolates in presence of an $^{\bullet}OH$ scavenger, $\Phi_{^1O_2}$ also increased close to linearly for low specific ozone doses (<0.35 $mmol_{O_3}$ $mmol_C^{-1}$) but leveled off for higher specific ozone doses.[3] This increase in $\Phi_{^1O_2}$ was attributed to the formation of quinones from the reaction of ozone with phenolic DOM moieties and the observed increase of $\Phi_{^1O_2}$ in Fig. 2 can most likely also be attributed to a formation of quinones.

The normalized (to the non-ozonated experiment) $\Phi_{^1O_2}$ in this study was compared to the data from ref. 3, where the ozonation was carried out in the presence of an $^{\bullet}OH$ scavenger (see Fig. S7, ESI†). The ratio of $\Phi_{^1O_2}$ from this study and the data from ref. 3 for PLFA is close to 1 for specific ozone doses up to 0.35 $mmol_{O_3}$ $mmol_C^{-1}$ and increases to 1.5 for a specific ozone dose of 0.5 $mmol_{O_3}$ $mmol_C^{-1}$ (see Fig. S7, ESI†). To determine if this specific ozone dose was anomalous, $\Phi_{^1O_2}$ was examined in detail by compiling the corresponding extent of $^1O_2$ production and extent of light absorption as a function of the ozone dose (see Table S3, ESI†). The increase to a value of 1.5 for a specific ozone dose of 0.5 $mmol_{O_3}$ $mmol_C^{-1}$ can be attributed to a decrease in the extent of $^1O_2$ production.[3] Ref. 3 presents additional specific ozone doses, which confirm that this observation is reproducible. Therefore, the observed value of a ratio of 1.5 observed in Fig. S7 (ESI†) is not an outlier. For SRFA, the ratio decreases to a value of 0.7 for specific ozone doses up to 0.15 $mmol_{O_3}$ $mmol_C^{-1}$ and then increases to 1.5 for specific ozone doses between 0.15 and to 0.5 $mmol_{O_3}$ $mmol_C^{-1}$.

The increase in the normalized quantum yield ratio to 1.5 for higher specific ozone doses can likely be attributed to the reaction of $^{\bullet}OH$ with non-activated aromatics, which are less reactive to ozone. For the experiments in presence of a $^{\bullet}OH$ scavenger, the pool of chromophores that are non-reactive towards ozone are maintained and should overall have a lower $\Phi_{^1O_2}$ than the pool of ozonated chromophores. Alternatively, in the present study in absence of a $^{\bullet}OH$ scavenger, the pool of ozone-resistant chromophores should react with $^{\bullet}OH$ to produce phenols and then quinones upon reaction with ozone,[15] which have a higher $\Phi_{^1O_2}$.

Effects of ozonation on the $^{\bullet}OH$ generation potential of DOM during UV irradiation

An approach similar to the $\Phi_{^1O_2}$ experiments was chosen to elucidate the factors influencing $\Phi_{^{\bullet}OH}$ upon ozonation. The light absorbed by the two DOM types (quantified by $SUVA_{avg}$) decreases dramatically as a function of the specific ozone dose (Fig. 2A). Fig. 3A shows that the rate of $^{\bullet}OH$ production upon irradiation, $r_{^{\bullet}OH}$, is fairly constant with increasing specific ozone doses for PLFA, while for SRFA it first increases for specific ozone doses ≤0.2 $mmol_{O_3}$ $mmol_C^{-1}$ and then decreases for higher specific ozone doses. Because $SUVA_{avg}$ is decreasing while $r_{^{\bullet}OH}$ remains fairly constant with increasing specific ozone doses, it can be concluded that $\Phi_{^{\bullet}OH}$ is increasing, similarly to $\Phi_{^1O_2}$. This is confirmed in Fig. 3B, with a significant increase in $\Phi_{^{\bullet}OH}$ for PLFA (by a factor of 28) and for SRFA (by a factor of 8.6) when the specific ozone dose increases from 0–0.5 $mmol_{O_3}$ $mmol_C^{-1}$.

The formation pathway of $^{\bullet}OH$ upon DOM irradiation is not entirely elucidated and many pathways have been proposed, which are summarized in a recent review.[11] Two main mechanisms are usually considered, H_2O_2-dependent and H_2O_2-independent pathways. The H_2O_2-dependent pathways involve Fenton and photo-Fenton chemistry and account for up

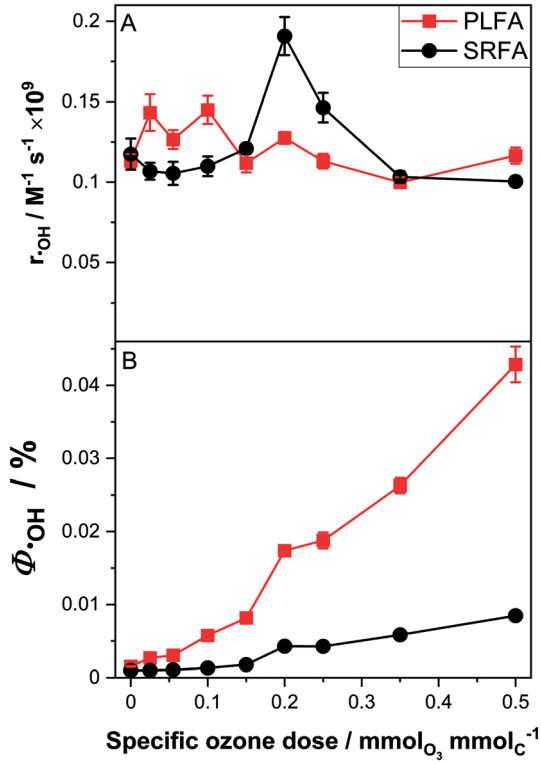

Fig. 3 UV irradiation of DOM: effects of the specific ozone dose on (A) the hydroxyl radical (˙OH) production rate ($r_{\cdot OH}$) and (B) the ˙OH quantum yield ($\Phi_{\cdot OH}$) for Pony Lake and Suwannee River fulvic acid (PLFA and SRFA, respectively). Red squares/lines: PLFA; black circles/lines: SRFA at a concentration of 5 mg_C L^{-1}. Solutions were buffered with 10 mM phosphate at pH 7, without hydroxyl radical scavenger. Error bars represent standard errors obtained from pseudo-first order fittings (BA experiments in duplicate). Lines are shown to guide the eye.

to 50% of the ˙OH production in some samples.[42,43] A variety of possibilities have been proposed for the H_2O_2-independent pathways. They include the photolysis of hydroxy substituted benzoic acids and phenols[44] and the oxidation of water or hydroxide ions by ^{3}DOM*, a mechanism that was seen to take place for a few photosensitizers such as 1-nitronaphthalene or anthraquinone-2,6-disulfonate.[45–47] If the production of ˙OH was due only to the photolysis of hydroxy substituted benzoic acids and phenols, one would expect $\Phi_{\cdot OH}$ to decrease upon ozonation due to the reaction and decomposition of the phenolic DOM moieties with ozone.[4,15,16,48] The observed increase in $\Phi_{\cdot OH}$ indicates that the source of ˙OH is probably the oxidation of water or hydroxide ions by ^{3}DOM*, or the formation of H_2O_2 during ozonation, which could induce the H_2O_2-dependent pathway.

The one-electron oxidation potentials of water and hydroxide are −2.73 V and −1.90 V respectively.[49] Quinones are known to have a high intersystem crossing yield and under photoirradiation form triplets that have a one-electron reduction potential in the range of 2.2–2.4 V (ref. 9) which is high enough to react with hydroxide and potentially with water. Therefore, it is hypothesized that the observed increase in $\Phi_{\cdot OH}$ could be attributed to the formation of quinones, which are common products from the reactions of ozone with hydroxylated aromatic compounds (*e.g.*, phenols).[4,15,16,48] It should be noted that for non-ozonated DOM, the photolysis of hydroxy substituted benzoic acids and phenols should not be excluded as a ˙OH source. A scenario for which ozonation increases the ˙OH production from DOM quinone moieties and decreases the production of ˙OH from the photolysis of substituted benzoic acid and phenols is also possible.

In studies on the oxidation of water or hydroxide ions by ^{3}DOM*, it has been shown that some other hydroxylating species (˙OH-like) are also generated, that have similar hydroxylating properties as ˙OH but lower reactivity.[42] Experiments involving photosensitizers indicate that some of them produce ˙OH,[45,50] but that for some photosensitizers, irradiation yielded species that were assigned to sensitizer-water exciplexes that could potentially be ˙OH-like species.[46,51–53]

It should be noted that the probe used to quantify ˙OH in our experiments, BA, could potentially also react with ˙OH-like species[42,52] and that part of the ˙OH measured in the experiments presented in Fig. 3 could be caused by ˙OH-like species.

Qualitative assessment of the production of ˙OH and of other hydroxylating species (˙OH-like). To qualitatively assess the potential formation of ˙OH-like species upon DOM ozonation, we designed the following competition kinetic experiment using BA as a probe and methanol as an ˙OH scavenger (it should be noted that it is also possible to quantify the formation of ˙OH using methanol but we only used it as a scavenger here). The assumption of these experiments is that the ratio $\frac{k_{BA,\cdot OH}}{k_{MeOH,\cdot OH}}$ (where $k_{BA,\cdot OH}$ = 5.9 × 10^9 M^{-1} s^{-1} or $k_{MeOH,\cdot OH}$ = 9.7 × 10^8 M^{-1} s^{-1} are the second-order rate constants for the reactions between BA or methanol and ˙OH, respectively)[20] will be different than the ratio $\frac{k_{BA,\cdot OH\text{-like}}}{k_{MeOH,\cdot OH\text{-like}}}$ (where $k_{BA,\cdot OH\text{-like}}$ and $k_{MeOH,\cdot OH\text{-like}}$ are the second-order rate constants for the reactions between BA or methanol and ˙OH-like species, respectively). The methanol quenching experiments were modeled using eqn (8), where f is the fraction of ˙OH reacting with BA, $k_{DOM,\cdot OH}$ are the second-order constants between DOM and ˙OH (4.6 × 10^8 and 1.9 × 10^8 M_C^{-1} s^{-1} for PLFA and SRFA respectively[54]) and $k_{NO_2^-,\cdot OH}$ is the second-order rate constant for the reaction between nitrite and ˙OH (1 × 10^{10} M^{-1} s^{-1} (ref. 20)).

$$f = \frac{k_{BA,\cdot OH}[BA]}{k_{BA,\cdot OH}[BA] + k_{MeOH,\cdot OH}[MeOH] + k_{DOM,\cdot OH}[DOM] + k_{NO_2^-,\cdot OH}[NO_2^-]} \quad (8)$$

Note that the reactions of ˙OH with the phosphate buffer and carbonate/bicarbonate from atmospheric CO_2 were neglected, as the fractional consumption of ˙OH by these components was small (f value <0.0001 for the phosphate buffer and <0.01 for the carbonate/bicarbonate, considering saturation conditions at 20 °C for the carbonate/bicarbonate concentration).

A control experiment was performed where nitrite was used as an alternative source of ˙OH to confirm the validity of eqn (8) and to verify that methanol acts as an ideal quencher (a potential drawback of the use of methanol is that its reaction with ˙OH produces $O_2^{\cdot-}$ quantitatively,[1] and $O_2^{\cdot-}$ disproportionation forms H_2O_2 that is potentially an additional source of ˙OH in the system).

Fig. 4 presents the normalized (to [methanol] = 0) rate of SA production. Fig. 4A shows that eqn (8) accurately describes the experiments performed with the photolysis of nitrite as a source of ˙OH. In Fig. 4B and C, a deviation from eqn (8) is observed, indicating that BA is not only reacting with ˙OH in the system. In contrast, ˙OH-like species might also be produced and involved in BA abatement. The ratio of the calculated value from eqn (8) over the experimental value is 1 for the nitrite control experiment. For PLFA the ratio is fairly constant for all specific ozone doses with a mean value of 0.47 for the non-ozonated samples and 0.46 and 0.55 for specific ozone doses of 0.2 and 0.5 $mmol_{O_3}$ $mmol_C^{-1}$, respectively. For SRFA the ratio is 0.66 for the non-ozonated samples and 0.48 and 0.92 for specific ozone doses of 0.2 and 0.5 $mmol_{O_3}$ $mmol_C^{-1}$, respectively.

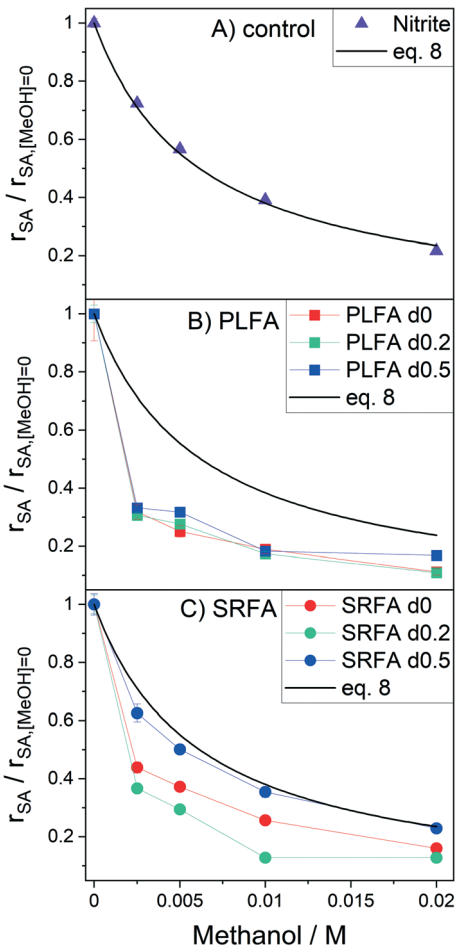

Fig. 4 Normalized salicylic acid (SA) production rate as a function of the methanol concentration. (A) Control nitrite experiment (violet, 6 μM $NaNO_2$). (B) Pony Lake fulvic acid (PLFA) treated with specific ozone doses of 0, 0.2 and 0.5 $mmol_{O_3}$ $mmol_C^{-1}$. (C) Suwannee River fulvic acid (SRFA) treated with specific ozone doses of 0, 0.2 and 0.5 $mmol_{O_3}$ $mmol_C^{-1}$. The black lines represent the fraction of ˙OH reacting with BA according to eqn (8). Benzoic acid concentration 1 mM, carbon concentration 5 mg_C L^{-1}. Solutions were buffered with 10 mM phosphate at pH 7. Lines are shown to guide the eye.

Comparison between the effects of ozonation on the generation potential of $^1O_2$ and ˙OH during UV irradiation

The measured $\Phi_{^1O_2}$ values were approximatively two orders of magnitude higher than $\Phi_{\cdot OH}$. This reflects the fact that $^1O_2$ is formed by oxygen reacting with ^{3}DOM* (eqn (3)) with an efficiency that was evaluated to be approximately 30%,[55] while ˙OH can be formed through several pathways that are relatively inefficient (*vide supra*).

A comparison of $\Phi_{^1O_2}$ and $\Phi_{\cdot OH}$ (Fig. 5) shows that the two quantum yields increase significantly with increasing specific ozone doses. Fig. 5A shows that $\Phi_{\cdot OH}$ and $\Phi_{^1O_2}$ increase more for PLFA than for SRFA. Plotting $\frac{\Phi_{\cdot OH,O_3}}{\Phi_{\cdot OH,O_3=0}} / \frac{\Phi_{^1O_2,O_3}}{\Phi_{^1O_2,O_3=0}}$ (*i.e.*, the relative ratio of increases of the two quantum yields; Fig. 5B) indicates that for PLFA, the increase in $\Phi_{\cdot OH}$ is more important than for $\Phi_{^1O_2}$, while for SRFA the ratio of increase of the two quantum yields is near unity for most specific ozone doses except for 0.2 and 0.25 $mmol_{O_3}$ $mmol_C^{-1}$, where higher ratios were observed.

The observed increase in $\Phi_{^1O_2}$ was attributed to the formation of quinones from the ozonation of phenolic DOM moieties. Only a relatively small subset of DOM chromophores produces ˙OH. The relative increase in $\Phi_{\cdot OH}$ is related to either a selective destruction of DOM chromophores that do not produce ˙OH or the formation of new DOM moieties that can produce ˙OH. An example of such new DOM moieties is quinones that are formed during ozonation and that under photoirradiation form triplets that have potentially high enough triplet one-electron oxidation potential to form ˙OH from water or hydroxide ions (see above).

Based on the current understanding of DOM photochemistry, it is difficult to develop an overarching model that explains the results observed in this study, as well as in other investigations by the authors. It is possible that

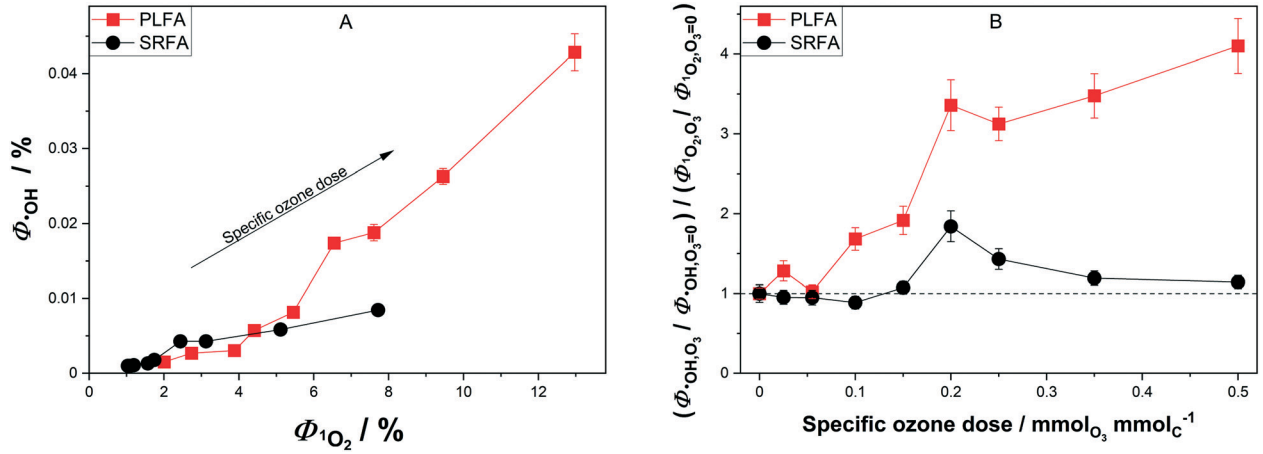

Fig. 5 Comparison between the effects of ozonation on the hydroxyl radical quantum yield ($\Phi_{\cdot OH}$) and the singlet oxygen quantum yield ($\Phi_{^1O_2}$) for Pony Lake and Suwannee River fulvic acids (PLFA and SRFA, respectively). (A) $\%\Phi_{\cdot OH}$ *vs.* $\%\Phi_{^1O_2}$. (B) Ratio of the normalized (to a specific ozone dose of 0 $mmol_{O_3}$ $mmol_C^{-1}$) $\Phi_{\cdot OH}$ over the normalized (to a specific ozone dose of 0 $mmol_{O_3}$ $mmol_C^{-1}$) $\Phi_{^1O_2}$ as a function of the specific ozone dose. Red squares/lines: PLFA; black circles/lines: SRFA. DOM at concentrations of 5 mg_C L^{-1}. Solutions were buffered with 10 mM phosphate at pH 7, without hydroxyl radical scavenger. Error bars represent standards errors obtained from the pseudo-first order fittings (FFA or BA experiments in duplicate). Lines are shown to guide the eye.

the results observed in this study are explained by the recalcitrance of quinone-derivatives to transformation by ozone and $^{\cdot}OH$. However, it is not clear if the photochemistry of quinones results in direct $^{\cdot}OH$ formation or the formation of $^{\cdot}OH$-like species and the relative efficiency of these two processes. It is also not clear how hydroxylation of quinones would affect $^1O_2$ formation.

In a previous study, we had also observed a positive correlation between the fluorescence quantum yield and the yield for the formation of $^1O_2$ during pre-ozonation in the presence of an $^{\cdot}OH$ scavenger.[3] Although we did not measure the fluorescence quantum yield in the current study, we expect that the same positive relationship would apply. Given that quinones are not fluorescent, it is unclear whether these observed correlations have any causational basis. More work is needed to ascertain these intercorrelations.

Conclusion

This study focused on the effects of ozonation on the optical and photochemical properties of two DOM types. Ozonation induced a significant decrease in DOM light absorbance properties and significant increases in the quantum yields of singlet oxygen ($\Phi_{^1O_2}$) and hydroxyl radical ($\Phi_{\cdot OH}$). For SRFA, the $\Phi_{\cdot OH}$ was observed to increase similarly to $\Phi_{^1O_2}$, while for PLFA the increase in $\Phi_{\cdot OH}$ was approximately four times larger than the observed increase in $\Phi_{^1O_2}$. The increases in $\Phi_{^1O_2}$ and $\Phi_{\cdot OH}$ were linked to the reactions of phenolic DOM moieties with ozone, which lead to the formation of quinones. The simultaneous use of a $^{\cdot}OH$ probe and a $^{\cdot}OH$ scavenger allowed for the distinction between the formation of $^{\cdot}OH$ and of other hydroxylating species ($^{\cdot}OH$-like species).

Overall, ozonation leads to an important decrease in the light absorption properties of DOM, which makes it a useful pre-treatment for UV-based treatment since the transparency of the water increases. For municipal wastewaters, where ozonation is used as a polishing step before discharge, the results of this study indicate that ozonation improves the visual aesthetics of the treated wastewater and also increases the potential for $^1O_2$- and $^{\cdot}OH$-induced reactions.

Conflicts of interest

The authors declare no competing financial interest.

Acknowledgements

Funding for this study came from the US National Science Foundation (1808126, 1833421, and 1549387). Funding from the University of Colorado SMART and Discovery Learning Assistantships programs is also acknowledged.

References

1 C. von Sonntag and U. von Gunten, *Chemistry of Ozone in Water and Wastewater Treatment: From Basic Principles to Applications*, IWA Publishing, London, UK, 2012.
2 R. I. Eggen, J. Hollender, A. Joss, M. Scharer and C. Stamm, Reducing the Discharge of Micropollutants in the Aquatic Environment: the Benefits of Upgrading Wastewater Treatment Plants, *Environ. Sci. Technol.*, 2014, **48**(14), 7683–7689.
3 F. Leresche, G. McKay, T. Kurtz, U. von Gunten, S. Canonica and F. L. Rosario-Ortiz, Effects of Ozone on the Photochemical and Photophysical Properties of Dissolved Organic Matter, *Environ. Sci. Technol.*, 2019, **53**(10), 5622–5632.
4 L. Önnby, E. Salhi, G. McKay, F. L. Rosario-Ortiz and U. von Gunten, Ozone and Chlorine Reactions with Dissolved Organic Matter - Assessment of Oxidant-Reactive Moieties by Optical Measurements and the Electron Donating Capacities, *Water Res.*, 2018, **144**, 64–75.

5 J. Wenk, M. Aeschbacher, E. Salhi, S. Canonica, U. von Gunten and M. Sander, Chemical Oxidation of Dissolved Organic Matter by Chlorine Dioxide, Chlorine, and Ozone: Effects on its Optical and Antioxidant Properties, *Environ. Sci. Technol.*, 2013, **47**(19), 11147–11156.

6 L. J. Fono, E. P. Kolodziej and D. L. Sedlak, Attenuation of Wastewater-Derived Contaminants in an Effluent-Dominated River, *Environ. Sci. Technol.*, 2006, **40**(23), 7257–7262.

7 M. Link, P. C. von der Ohe, K. Voss and R. B. Schafer, Comparison of Dilution Factors for German Wastewater Treatment Plant Effluents in Receiving Streams to the Fixed Dilution Factor from Chemical Risk Assessment, *Sci. Total Environ.*, 2017, **598**, 805–813.

8 K. Fenner, S. Canonica, L. P. Wackett and M. Elsner, Evaluating Pesticide Degradation in the Environment: Blind Spots and Emerging Opportunities, *Science*, 2013, **341**(6147), 752–758.

9 K. McNeill and S. Canonica, Triplet State Dissolved Organic Matter in Aquatic Photochemistry: Reaction Mechanisms, Substrate Scope, and Photophysical Properties, *Environ. Sci.: Processes Impacts*, 2016, **18**(11), 1381–1399.

10 C. Richard and S. Canonica, Aquatic Phototransformation of Organic Contaminants Induced by Coloured Dissolved Natural Organic Matter, in *Handbook of Environmental Chemistry*, Springer-Verlag, Berlin, Germany, 2005, vol. 2, pp. 299–323.

11 D. Vione, M. Minella, V. Maurino and C. Minero, Indirect Photochemistry in Sunlit Surface Waters: Photoinduced Production of Reactive Transient Species, *Chemistry*, 2014, **20**(34), 10590–10606.

12 J. Hoigné, B. C. Faust, W. R. Haag, F. E. Scully and R. G. Zepp, Aquatic Humic Substances as Sources and Sinks of Photochemically Produced Transient Reactants, *Adv. Chem. Ser.*, 1989, **219**, 363–381.

13 S. Mostafa and F. L. Rosario-Ortiz, Singlet Oxygen Formation from Wastewater Organic Matter, *Environ. Sci. Technol.*, 2013, **47**(15), 8179–8186.

14 E. C. Wert, F. L. Rosario-Ortiz, D. D. Drury and S. A. Snyder, Formation of Oxidation Byproducts from Ozonation of Wastewater, *Water Res.*, 2007, **41**(7), 1481–1490.

15 P. R. Tentscher, M. Bourgin and U. von Gunten, Ozonation of *Para*-Substituted Phenolic Compounds Yields *p*-Benzoquinones, Other Cyclic α,β-Unsaturated Ketones, and Substituted Catechols, *Environ. Sci. Technol.*, 2018, **52**(8), 4763–4773.

16 E. Mvula and C. von Sonntag, Ozonolysis of phenols in aqueous solution, *Org. Biomol. Chem.*, 2003, **1**(10), 1749–1756.

17 R. Flyunt, A. Leitzke, G. Mark, E. Mvula, E. Reisz, R. Schick and C. von Sonntag, Determination of $^{\bullet}OH$, $O_2^{\bullet-}$, and Hydroperoxyde Yield in Ozone Reaction in Aqueous Solution, *J. Phys. Chem. B*, 2003, **107**(30), 7242–7253.

18 M. O. Buffle and U. von Gunten, Phenols and Amine Induced $HO^{\bullet}$ Generation During the Initial Phase of Natural Water Ozonation, *Environ. Sci. Technol.*, 2006, **40**(9), 3057–3063.

19 T. Nöthe, H. Fahlenkamp and C. von Sonntag, Ozonation of Wastewater: Rate of Ozone Consumption and Hydroxyl Radical Yield, *Environ. Sci. Technol.*, 2009, **43**(15), 5990–5995.

20 G. V. Buxton, C. L. Greenstock, W. P. Helman and A. B. Ross, Critical-Review of Rate Constants for Reactions of Hydrated Electrons, Hydrogen-Atoms and Hydroxyl Radicals ($^{\bullet}OH/^{\bullet}O^{-}$) in Aqueous-Solution, *J. Phys. Chem. Ref. Data*, 1988, **17**(2), 513–886.

21 D. O. Mártire, C. Evans, S. G. Bertolotti, S. E. Braslavsky and N. A. Garcia, Singlet Molecular-Oxygen Production and Quenching by Hydroxybiphenyls, *Chemosphere*, 1993, **26**(9), 1691–1701.

22 F. Wilkinson, W. P. Helman and A. B. Ross, Quantum Yields for the Photosensitized Formation of the Lowest Electronically Excited Singlet-State of Molecular-Oxygen in Solution, *J. Phys. Chem. Ref. Data*, 1993, **22**(1), 113–262.

23 R. Schmidt, C. Tanielian, R. Dunsbach and C. Wolff, Phenalenone, a Universal Reference Compound for the Determination of Quantum Yield of Singlet Oxygen Sensitization, *J. Photochem. Photobiol., A*, 1994, **79**(1–2), 11–17.

24 C. Marti, O. Jurgens, O. Cuenca, M. Casals and S. Nonell, Aromatic ketones as standards for singlet molecular oxygen photosensitization. Time-resolved photoacoustic and near-IR emission studies, *J. Photochem. Photobiol., A*, 1996, **97**(1–2), 11–18.

25 I. Gutiérrez, S. G. Bertolotti, M. A. Biasutti, A. T. Soltermann and N. A. Garcia, Quinones and hydroxyquinones as generators and quenchers of singlet molecular oxygen, *Can. J. Chem.*, 1997, **75**(4), 423–428.

26 M. Bourgin, B. Beck, M. Boehler, E. Borowska, J. Fleiner, E. Salhi, R. Teichler, U. von Gunten, H. Siegrist and C. S. McArdell, Evaluation of a Full-Scale Wastewater, Treatment Plant Upgraded with Ozonation and Biological Post-Treatments: Abatement of Micropollutants, Formation of Transformation Products and Oxidation By-Products, *Water Res.*, 2018, **129**, 486–498.

27 J. Hollender, S. G. Zimmermann, S. Koepke, M. Krauss, C. S. McArdell, C. Ort, H. Singer, U. von Gunten and H. Siegrist, Elimination of Organic Micropollutants in a Municipal Wastewater Treatment Plant Upgraded with a Full-Scale Post-Ozonation Followed by Sand Filtration, *Environ. Sci. Technol.*, 2009, **43**(20), 7862–7869.

28 S. G. Zimmermann, M. Wittenwiler, J. Hollender, M. Krauss, C. Ort, H. Siegrist and U. von Gunten, Kinetic Assessment and Modeling of an Ozonation Step for Full-Scale Municipal Wastewater Treatment: Micropollutant Oxidation, By-Product Formation and Disinfection, *Water Res.*, 2011, **45**(2), 605–617.

29 F. Hammes, E. Salhi, O. Koster, H. P. Kaiser, T. Egli and U. von Gunten, Mechanistic and Kinetic Evaluation of Organic Disinfection By-Product and Assimilable Organic Carbon (AOC) Formation During the Ozonation of Drinking Water, *Water Res.*, 2006, **40**(12), 2275–2286.

30 F. L. Rosario-Ortiz and S. Canonica, Probe Compounds to Assess the Photochemical Activity of Dissolved Organic Matter, *Environ. Sci. Technol.*, 2016, **50**(23), 12532–12547.

31 E. Appiani, R. Ossola, D. E. Latch, P. R. Erickson and K. McNeill, Aqueous Singlet Oxygen Reaction Kinetics of Furfuryl Alcohol: Effect of Temperature, pH, and Salt Content, *Environ. Sci.: Processes Impacts*, 2017, **19**(4), 507–516.

32 J. G. Qian, K. Mopper and D. J. Kieber, Photochemical Production of the Hydroxyl Radical in Antarctic Waters, *Deep Sea Res., Part I*, 2001, **48**(3), 741–759.

33 D. Dulin and T. Mill, Development and Evaluation of Sunlight Actinometers, *Environ. Sci. Technol.*, 1982, **16**(11), 815–820.

34 J. R. Laszakovits, S. M. Berg, B. G. Anderson, J. E. O'Brien, K. H. Wammer and C. M. Sharpless, *p*-Nitroanisole/Pyridine and *p*-Nitroacetophenone/Pyridine Actinometers Revisited: Quantum Yield in Comparison to Ferrioxalate, *Environ. Sci. Technol. Lett.*, 2017, **4**(1), 11–14.

35 J. Peuravuori and K. Pihlaja, Molecular Size Distribution and Spectroscopic Properties of Aquatic Humic Substances, *Anal. Chim. Acta*, 1997, **337**(2), 133–149.

36 E. S. Boyle, N. Guerriero, A. Thiallet, R. Del Vecchio and N. V. Blough, Optical properties of humic substances and CDOM: relation to structure, *Environ. Sci. Technol.*, 2009, **43**(7), 2262–2268.

37 G. McKay, W. X. Huang, C. Romera-Castillo, J. E. Crouch, F. L. Rosario-Ortiz and R. Jaffe, Predicting Reactive Intermediate Quantum Yields from Dissolved Organic Matter Photolysis Using Optical Properties and Antioxidant Capacity, *Environ. Sci. Technol.*, 2017, **51**(10), 5404–5413.

38 L. M. Dorfman, D. A. Harter and I. A. Taub, Rate Constants for the Reaction of the Hydroxyl Radical with Aromatic Molecules, *J. Chem. Phys.*, 1964, **41**(9), 2954–2955.

39 J. R. Helms, A. Stubbins, J. D. Ritchie, E. C. Minor, D. J. Kieber and K. Mopper, Absorption Spectral Slopes and Slope Ratios as Indicators of Molecular Weight, Source, and Photobleaching of Chromophoric Dissolved Organic Matter, *Limnol. Oceanogr.*, 2008, **53**(3), 955–969.

40 R. M. Dalrymple, A. K. Carfagno and C. M. Sharpless, Correlations Between Dissolved Organic Matter Optical Properties and Quantum Yield of Singlet Oxygen and Hydrogen Peroxide, *Environ. Sci. Technol.*, 2010, **44**, 5824–5829.

41 B. M. Peterson, A. M. McNally, R. M. Cory, J. D. Thoemke, J. B. Cotner and K. McNeill, Spatial and Temporal Distribution of Singlet Oxygen in Lake Superior, *Environ. Sci. Technol.*, 2012, **46**(13), 7222–7229.

42 S. E. Page, W. A. Arnold and K. McNeill, Assessing the Contribution of Free Hydroxyl Radical in Organic Matter-Sensitized Photohydroxylation Reactions, *Environ. Sci. Technol.*, 2011, **45**(7), 2818–2825.

43 M. M. Dong and F. L. Rosario-Ortiz, Photochemical Formation of Hydroxyl Radical from Effluent Organic Matter, *Environ. Sci. Technol.*, 2012, **46**(7), 3788–3794.

44 L. N. Sun, J. G. Qian, N. V. Blough and K. Mopper, Insights into the Photoproduction Sites of Hydroxyl Radicals by Dissolved Organic Matter in Natural Waters, *Environ. Sci. Technol. Lett.*, 2015, **2**(12), 352–356.

45 B. Sur, M. Rolle, C. Minero, V. Maurino, D. Vione, M. Brigante and G. Mailhot, Formation of Hydroxyl Radicals by Irradiated 1-Nitronaphthalene (1NN): Oxidation of Hydroxyl Ions and Water by the 1NN Triplet State, *Photochem. Photobiol. Sci.*, 2011, **10**(11), 1817–1824.

46 J. N. Moore, D. Phillips, N. Nakashima and K. Yoshihara, Photochemistry of 9,10-Anthraquinone-2,6-disulphonate, *J. Chem. Soc., Faraday Trans.*, 1986, **82**, 745–761.

47 S. Garg, A. L. Rose and T. D. Waite, Production of Reactive Oxygen Species on Photolysis of Dilute Aqueous Quinone Solutions, *Photochem. Photobiol.*, 2007, **83**(4), 904–913.

48 M. K. Ramseier and U. von Gunten, Mechanisms of Phenol Ozonation-Kinetics of Formation of Primary and Secondary Reaction Products, *Ozone: Sci. Eng.*, 2009, **31**(3), 201–215.

49 D. A. Armstrong, R. E. Huie, W. H. Koppenol, S. V. Lymar, G. Merenyi, P. Neta, B. Ruscic, D. M. Stanbury, S. Steenken and P. Wardman, Standard Electrode Potentials Involving Radicals in Aqueous Solution: Inorganic Radicals (IUPAC Technical Report), *Pure Appl. Chem.*, 2015, **87**(11–12), 1139–1150.

50 T. Kitamura, H. Fudemoto, Y. Wada, K. Murakoshi, M. Kusaba, N. Nakashima, T. Majima and S. Yanagida, Visible Light Induced Photo-Oxidation of Water. Formation of Intermediary Hydroxyl Radicals through the Photoexcited Triplet State of Perfluorophenazine, *J. Chem. Soc., Faraday Trans.*, 1997, **93**(2), 221–229.

51 D. Gan, M. Jia, P. P. Vaughan, D. E. Falvey and N. V. Blough, Aqueous Photochemistry of Methyl-benzoquinone, *J. Phys. Chem. A*, 2008, **112**(13), 2803–2812.

52 A. Pochon, P. P. Vaughan, D. Q. Gan, P. Vath, N. V. Blough and D. E. Falvey, Photochemical Oxidation of Water by 2-Methyl-1,4-benzoquinone: Evidence Against the Formation of Free Hydroxyl Radical, *J. Phys. Chem. A*, 2002, **106**(12), 2889–2894.

53 I. Loeff, A. Treinin and H. Linschitz, Photochemistry of 9,10-Anthraquinone-2-Sulfonate in Solution. 1. Intermediates and Mechanism, *J. Phys. Chem.*, 1983, **87**(14), 2536–2544.

54 E. Appiani, S. E. Page and K. McNeill, On the Use of Hydroxyl Radical Kinetics to Assess the Number-Average Molecular Weight of Dissolved Organic Matter, *Environ. Sci. Technol.*, 2014, **48**(20), 11794–11802.

55 M. Schmitt, P. R. Erickson and K. McNeill, Triplet-State Dissolved Organic Matter Quantum Yields and Lifetimes from Direct Observation of Aromatic Amine Oxidation, *Environ. Sci. Technol.*, 2017, **51**(22), 13151–13160.

